

Structure of Nuclei in Strong Magnetic Fields

V. N. Kondratyev*

Advanced Science Research Center, Japan Atomic Energy Research Institute, Tokai, Ibaraki 319-1195, Japan

Received: November 13, 2001; In Final Form: November 13, 2001

The structure of nuclei in ultrastrong magnetic fields relevant for supernovas and neutron stars is considered. The dependence of shell-correction energy on magnetic field is analyzed and systemized by employing the shell model with spherical harmonic oscillator confining potential.

1. Introduction

The astrophysical environment can affect significantly properties of nuclides. In particular, the structure of nuclei can be dramatically modified¹ by ultrastrong magnetic fields leading, e.g., to a shift of nuclear magic numbers. The related field strengths $B \sim 10^{15} - 10^{17}$ G correspond to a flux $\Phi_0 \sim \hbar c / \pi e$ through an area covered by the size of nuclei and can be met, e.g., in supernovas and neutron stars. Many observations, like short bright outbursts of soft gamma repeaters (SGRs)^{2,3} and rapid braking of relatively slowly rotating stars associated with SGRs^{4,5} and anomalous X-ray pulsars (AXPs),^{6,7} provide evidences in support of such ‘magnetar’ concept^{8–10} implying ultra-magnetized stellar media with fields of a strength ranging up to $B \sim 10^{17.5}$ G. Consequently, the nuclear synthesis in the vicinity of supernova core can be noticeably affected by the magnetic field of respective nascent neutron star. Such transformations of nuclide structure can play an important role also in magneto-transport of neutron star crusts¹¹ and contribute to some specific features of magnetic emission, like soft gamma-ray bursts.¹²

The inhomogeneous (crusty) nuclear matter at densities \mathcal{D} less than the saturation density \mathcal{D}_s has been extensively studied theoretically (cf. References 13–17 and references therein). The outer crusts is viewed to be composed from well separated nuclei with the largest binding energy. The shell closure in iron region determines such a bottom of fusion and fission valleys in laboratory.¹⁸ With increasing nuclear density large mass magic numbers grow in importance, so that the nucleon aggregates of masses matching the superheavy sector might be expected to be naturally abundant in crust inner regions.^{16,17} The star activity related to a change of nuclear structure in, e.g., evolving magnetic fields can be employed, indeed, to probe properties of nuclei as well as crust magnetodynamics.

In this contribution we analyze general features of the field induced modification of the shell effect for large mass nuclei. In sect. 2 we briefly recall mean-field treatment applied for the description of nuclear magnetism and systemize the properties of spin- and orbital magnetic response of neutrons and protons. The conclusions are in sect. 3.

2. Magnetism of Nuclei within the Shell Model

As demonstrated by Kondratyev et al.¹ thermodynamic formalism within the non-relativistic mean-field treatment constitutes useful framework for an analysis of the nuclide reactivity in magnetic fields of interest. Relativistic effects become important at considerably larger field strengths when the energy of the first Landau level $\omega_L = \mu_N B$ (with the nuclear magneton μ_N) becomes comparable to the nucleon rest mass. The magnitude of the respective limiting field for nucleons $B_{\text{rel}}^N = m_p c^2 / 2\mu_N \approx 1.5 \times 10^{20}$ G corresponds to a flux $\Phi_0 = \hbar c / \pi e$ through the area of a radius given by the nucleon Compton

wavelength $\lambda_N = \hbar / (m_p c) \approx 0.21$ fm. These fields may affect, e.g., conditions of β -equilibrium of the neutron star bulk matter.¹⁹

Within the Hartree mean-field treatment (see, e.g., References 1, 20, 21) the nuclear structure is described in terms of the filled up to the Fermi energy ϵ_F single-particle (sp) levels ϵ_ζ , which determine the properties of $N = \int_{-\infty}^{\epsilon_F} d\epsilon \rho(\epsilon)$ nucleons. Decomposing the sp level density $\rho(\epsilon) = \sum_\zeta \delta(\epsilon - \epsilon_\zeta) = \rho^{\text{sm}} + \delta\rho$ into smooth ρ^{sm} and oscillating $\delta\rho$ components we express the energy of a nucleus as

$$E = \int_{-\infty}^{\epsilon_F} d\epsilon \epsilon \rho(\epsilon) = E^{\text{sm}} + \delta E_n + \delta E_p, \quad (1)$$

where the Thomas-Fermi (i.e. semi-classical) component E^{sm} is only slightly affected by magnetic fields due to the Bohr-van Leeuwen theorem.²² The leading field effect is connected with shell-correction contributions^{1,23} of neutrons δE_n and protons δE_p to nuclear masses which are related to the oscillating part $\delta\rho$.

Great success in the understanding of many properties of stable nuclei is associated with the Nilsson model (NM) (cf. e.g. References 20, 21) which is based on the Harmonic Oscillator (HO) confining potential approximation for the nuclear mean-field. In present study we consider the simple spherical HO Hamiltonian yielding the equidistant sp spectrum

$$\epsilon_n = (n + 3/2) \quad (2)$$

corresponding to principal quantum numbers n with level degeneracies $(n + 1)(n + 2)$, and measured in units of the HO frequency ω_0 . For nuclei in vicinity of stability line $\omega_0 \approx 41/A^{1/3}$ MeV, while neutron rich nuclei of crust inner region correspond to significantly smaller level spacing. Consequently, such a picture of HO confinement might provide reliable description of inner crust nuclides with considerably suppressed spin-orbit (s-o) coupling.^{14,15}

2.1. Pauli-spin Magnetization. The interaction of magnetic field with nucleon-spin-dipole magnetic moment leads to an additional term in the energy spectra

$$\delta\epsilon_i = \sigma_i \Delta_\alpha, \quad \Delta_\alpha = g_\alpha b / 2 \quad (3)$$

with the g-factor g_α , and reduced field strength $b = \omega_L / \omega_0$. Such a term contributes to sp energies of both protons $\alpha = p$, and neutrons $\alpha = n$, and gives rise to a relative shift down and up (see Figure 1b) of energy levels with the nucleon spin-magnetic moment directed along the field ($\sigma_{i=\uparrow} = -1$, majority-spin levels) and in the opposite direction ($\sigma_{i=\downarrow} = 1$, minority-spin levels), respectively. The shift, eq 3, is related to the Pauli-type of the magnetic response and modifies the shell-correction energy as

$$\delta E_\alpha = \delta E_\alpha^\uparrow(\epsilon_F + \Delta_\alpha) + \delta E_\alpha^\downarrow(\epsilon_F - \Delta_\alpha), \quad (4)$$

where δE_α^i is determined by the unshifted sp spectrum (see eq 1, 2).

*E-mail: vkondra@hadron03.tokai.jaeri.go.jp. FAX: +81-29-282-5927.

The spin magnetization represents predominant effect in the magnetic field dependence of the neutron shell-correction energy and leads to a phase-shift of shell-oscillations.¹ This behavior is caused by the field dependent interference of contributions coming from the majority- and minority-spin neutrons to the total energy. As illustrated in Figure 1a such an interference gives rise to oscillations of the shell-energy as a function of magnetic field strength with a period $b_s \approx 0.5$. Figure 1b indicates that for nearly stable nuclei the respective magnetic field $B_s \sim \omega_0/\mu_N \sim 10^{16}-10^{17}$ G induces the relative shift Δ_n , eq 3, of neutron majority- and minority-spin energy levels which is comparable to the energy difference between major shells given by the HO frequency ω_0 . In particular, at field strengths corresponding to the region near $b \approx |2g_n|^{-1} \approx 0.26$ the level spacing and the degeneracies are decreased resulting in a suppression of the shell effect as compared to the values related to level crossings, $b_{cr} = |k/g_n|$ with an integer k .

At zero-field the pronounced minima are displayed at neutron numbers, $N_m^0 = 8, 20, 40, 70, 112, 168, \dots$, associated with closed shells, as extensively discussed in, e.g., Reference 20. In the case of $b \approx |1/g_n|$ the level spacing and the shell-oscillation am-

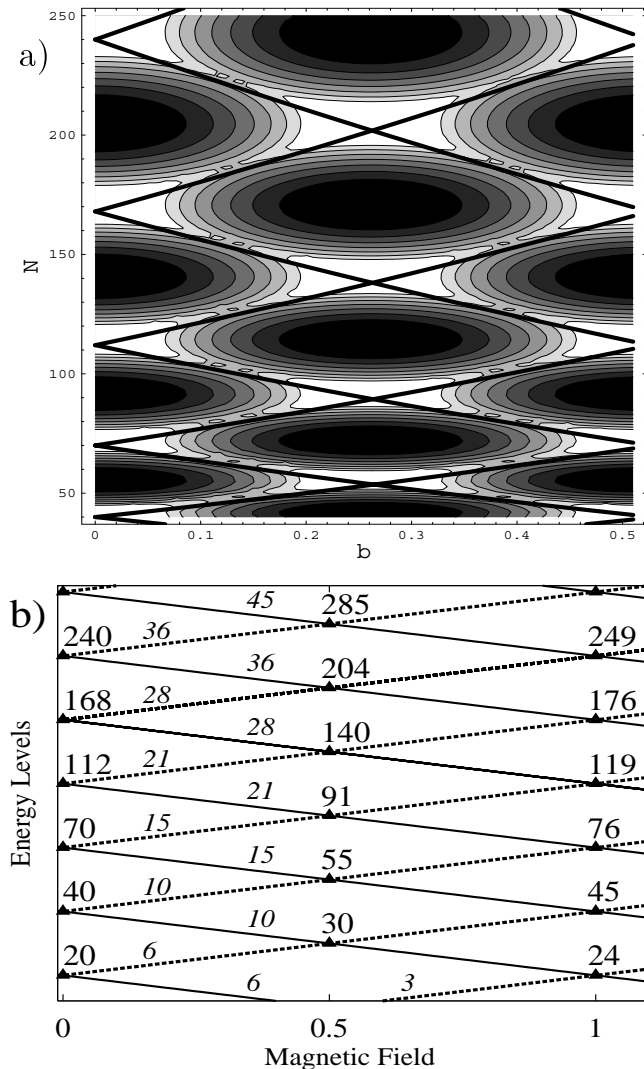


Figure 1. (a) Spherical HO model prediction of the neutron shell-correction energy versus the neutron number N and the parameter b . Smaller energies are indicated by white regions, while the dark regions denote larger energies. The contours are plotted with the step 0.5 starting from -1.5 for the quantity $\delta E_n \cdot 8\pi^4 / (\omega_0 X^2)$. The thick solid lines are related to the relationship eq 5. (b) The dependence of the majority- and minority-spin (dashed lines) energy level on the magnetic field. The energy and the field are measured in the units of the HO level spacing ω_0 and $[\omega_0/g_n\mu_N]$, respectively. The figures at the level crossings (indicated by triangles) show the total nucleon number when the levels are filled starting from the bottom. The level degeneracies are displayed by the numbers attached to respective lines.

plitude are nearly the same as at $b \approx 0$. However, as indicated in Figure 1b level occupation numbers are rather different in these two cases. Consequently, the positions of shell-energy minima are replaced. At the field strength matching the first level crossing the familiar spherical HO magic numbers are turned into anti-magic, i.e. associated with positive maxima of the shell-correction energy, while the open shell anti-magic numbers become the closed shell magic numbers. For grand canonical ensemble the field dependence of the shell energy minima can be obtained from the condition of constant arguments in eq 4. This yields an approximation

$$N_m^\pm / N_m^0 \approx (1 \mp g_n b / 2(3N_m^0)^{1/3})^3, \quad (5)$$

where \pm corresponds to upper and lower valleys extending from the respective zero-field magic numbers N_m^0 (see Figure 1a). As evident from Figure 1a linear term dominates such a dependence. We note that magic number of canonical ensemble deviate from the case of grand canonical by about 1% and 5% at the first and second level crossings, respectively.

The effect of a sign change in the shell-correction energy remains when accounting for the spin-orbit interaction as well.¹ Furthermore, the sign inversion occurs at the field strength that is almost an order of magnitude smaller than the oscillation period B_s (see above).

2.2. Orbital Magnetism. The interaction of magnetic field with moving along the confined trajectory proton charge gives rise to an additional modification of proton spectra which at small field strengths $b \ll 1$ reads

$$\delta \varepsilon_o \approx b l_3, \quad (6)$$

where l_3 denotes the projection of the proton angular momentum on the field axis. Switching off the Pauli response (i.e. $\Delta_p = 0$ in eq 4) the properties of the orbital magnetism can be easily seen by employing the simplified expression for the shell-correction energy at conditions of weak fields in the form (see References 1, 24)

$$\delta E_o^i \approx -\frac{\omega_0 X(X+1)}{8\pi^4} \sum_{k=1} k^{-2} \cos(kX) j_0(bkX), \quad (7)$$

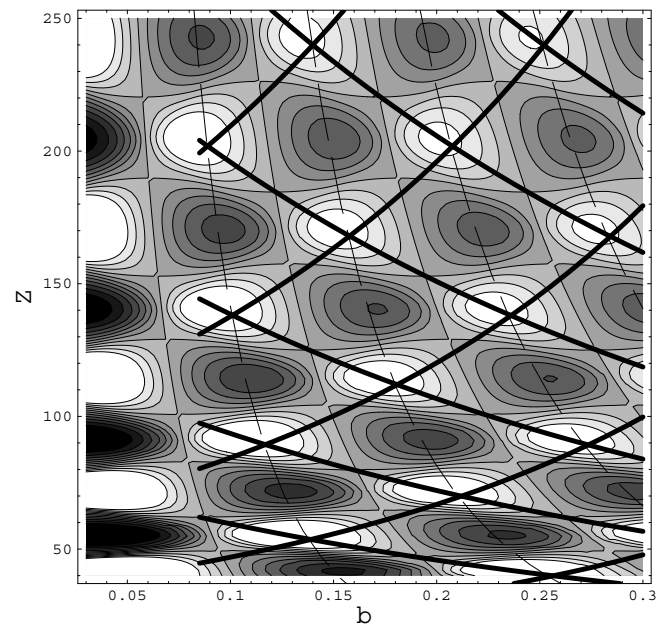


Figure 2. Effect of orbital magnetism in the proton shell-correction energy versus the proton number Z and the parameter b for the spherical HO potential. The white regions display to the energy minima (i.e. the wells), while the dark regions indicate the maxima (i.e. the hills) in the shell-correction energy landscape. The contours are plotted with the step 0.15 starting from -1 for the quantity $\delta E_p \cdot (1+b/b_0)8\pi^4 / (\omega_0 X^2)$, where $b_0 = (4 \cdot 90^{1/3})^{-1} \approx 0.056$. Thick solid lines represent eq 9, while dashed lines correspond to eq 8.

where $X = 2\pi\varepsilon_F/\omega_0 \approx 2\pi(3N)^{1/3}$ counts the number of filled shells in zero-field limit. The effect of orbital magnetism consists, therefore, in a modulation of components for a non-perturbed spherical HO by the spherical Bessel function with the field dependent argument. As indicated by eq 7 and illustrated in Figure 2 the weak field leads to regular oscillations of the shell-correction energy as a function of the field strength as well as overall suppression the shell effect with increasing b at zero s-o coupling. As seen in Figure 2 local maxima of the shell-energy amplitude arise along the lines

$$Z^p \approx [(p+1/2)/2b]^3/3 \quad (8)$$

with an integer p . The shell-correction component vanishes when in eq 8 $p = k + 1/2$ at integer k . Therefore, orbital magnetism yields the oscillation period $b_o \approx X^{-1} \sim A^{-1/3}$ corresponding to the field strength $B_o = \omega_0/\mu_N X \sim A^{-2/3}$. This estimate (cf. also Figure 2) yields a weaker field for heavier nuclei in order to invert the sign of the proton shell-correction energy as well as to wash out the shell-structure. The minima valleys in shell-correction energy landscape follow the lines

$$Z_m^\pm/Z_m^0 \approx [(1 \mp b_m)/(1 \mp b)]^3, \quad b_m = 1/(4(3Z_m^0)^{1/3}), \quad (9)$$

with a good accuracy up to the third oscillation.

2.3. Paramagnetism versus Orbital Magnetism of Protons in Nuclei. The magnetic field dependence of the proton shell-correction energy is given as a combination of the discussed in sect. 2.1, Figure 1 and eq 4, Pauli-magnetism and the Landau-type of orbital magnetism related to proton ballistic dynamics (see Figure 2 and eq 6, 7). Switching on the spin-magnetic response we obtain the proton shell-correction energy which is shown in Figure 3 as a function of the proton number Z and magnetic field strength b . As seen the damped oscillations of the shell energy correspond to the period b_{so} decreasing with the mass number similarly to a pure orbital magnetism. The Pauli-type magnetization reduces, however, additionally the field strength that is required to change the sign in the proton shell-correction energy. The phase-shift on π (i.e. the reversed sign) occurs at the parameter b which is considerably smaller than the value $1/g_p$. The interplay between the Landau-type and spin-magnetism gives rise to an extra-decrease of the period of a sign oscillation. The relevant field strength is, therefore,

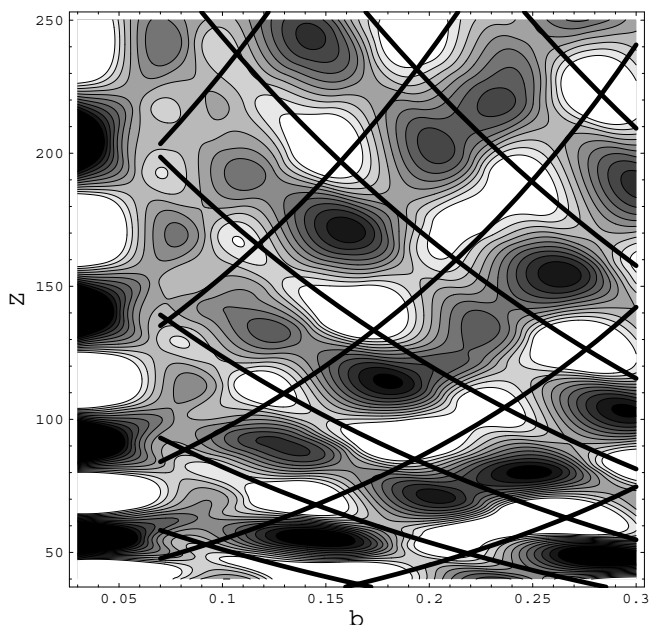


Figure 3. Spherical HO model prediction for the magnetic field dependent proton shell-correction energy when including spin and orbital magnetization. The contours are the same as in Figure 2, while thick solid lines are associated with eq 10.

smaller than the corresponding field for neutrons by a factor exceeding the ratio $|g_p/g_n|$. At the Fermi energy the respective magnetic field shifts the proton majority- and minority-spin levels on an energy $(\delta\varepsilon_i + \delta\varepsilon_o)$ comparable to the HO level spacing ω_0 . The energy of the first Landau level ω_L is, however, by the factor 6–7 smaller than the energy difference between the major shells, while the radius of the proton cyclotron orbit is larger than the radii of nuclei on approximately the same factor. Consequently, Landau levels give almost no contribution to the magnetism of nuclei. The orbital magnetism in such a case is mainly given by an interaction of the magnetic field with the magnetic dipole arising from the quantum orbital motion of protons inside the nucleus. The orbital magnetic response of such an inhomogeneous system is considerably amplified as compared to the magnetism of a homogeneous liquid which originates from the quantization of proton orbital motion in magnetic field. The Landau levels are expected to contribute noticeably to the magnetic response when their and nuclear radii become comparable. Corresponding field strength $B_L \sim 10^{19}$ G.

As seen from the comparison of Figures 1, 2 and 3 the interplay between spin and orbital magnetic reactivities yields more complicated proton shell-correction energy landscape as compared to their independent responses in a field. In this case the magnetic field evolution of the proton shell-energy valleys can be guided by the lines

$$Z_m^\pm/Z_m^0 \approx [(1 \mp b_m)/(1 \mp b)] \pm g_p b/2(3Z_m^0)^{1/3} \quad (10)$$

which represent a combination of eq 5, but with proton g-factor g_p , and eq 9. As illustrated in Figure 3 the valleys display irregular shapes passing from upper to lower lines.

It is worthy to recall here that the presence of s-o interaction leads, in addition, to an anomalous field dependence of the proton shell-correction energy amplitude.¹ The proton orbital magnetism yields rather pronounced enhancement of the shell effect. Especially, when the values of the parameter b are close to the spin-orbit strength, the shell-oscillation amplitude can be considerably amplified.

3. Conclusion

In summary, we have discussed an effect of ultrastrong magnetic fields on the structure of nuclei. As shown within the employed mean-field treatment such a field influence can be viewed as a shift of nucleon energy levels which is governed by the projection of respective magnetic moments on the field axis. Making use of the shell model with spherical HO confining potential we have analyzed common features of magnetic field dependence of shell-correction energy and magic numbers. For neutrons such effects entirely originate from the Pauli-type paramagnetic response. As a consequence, for equidistant HO spectrum the neutron shell-correction energy displays almost periodic behavior as a function of the magnetic field strength. As seen within the considered model the field evolution of valleys associated neutron magic numbers follow nearly straight lines corresponding to eq 5.

The interplay between spin- and orbital-magnetism determines the proton magnetic response. As demonstrated at zero spin-orbit interaction the Landau-type of orbital magnetic response results in a damped oscillations of the shell energy as a function of magnetic field. The overall amplitude of shell oscillations is inversely proportional to the magnetic field strength, while the amplitude maxima arise at the fields given by eq 8. The energy minima valleys associated with magic numbers follow the lines associated with eq 9. The combination of spin- and orbital magnetic response brings complicated shell correction energy landscape. The valleys of nuclear magics extend attaching upper and lower lines of eq 10, repeatedly.

As a matter of fact, the nuclear level density represents an important ingredient to the prediction of nuclear reaction cross

sections.²⁵ Therefore, our analysis indicates possible magnetic field dependence of the nuclear reaction (e.g. *s*- and *r*-processes) rates and, consequently, abundance of elements in, e.g., supernova remnants.

We note finally that similar shift of magic numbers can show up in, e.g., atomic clusters. The scale of the respective field strength for e.g. an alkaline cluster of N_{ac} atoms $B_{ac} \sim \epsilon_F^{ac} / (3N_{ac})^{1/3} \mu_B \sim 10^9 / (3N_{ac})^{1/3}$ G (with the Bohr magneton μ_B) suggests a possibility for laboratory tests of the predicted phase-shift of shell-oscillations.

Acknowledgments. The author is indebted to A. Iwamoto, Y. Abe, T. Tatsumi, S. Chiba, T. Maruyama, K. Niita, K. Oyamatsu, and M. Matsuzaki for valuable discussions and thanks the Research Group for Hadron Science at JAERI for the warm hospitality.

References

- (1) V. N. Kondratyev, T. Maruyama, and S. Chiba, JAERI-Research 99-065 (1999); Phys. Rev. Lett. **84**, 1086 (2000); JAERI-Review 2000-18, 61 (2000); JAERI-Conf 2000-11, 99 (2000); Astrophys. J. **546**, 1137 (2001); J. Nucl. Sci. Technol. (in press).
- (2) E. P. Mazets, S. V. Golenskii, V. N. Ilinskii, R. L. Aptekar, and Iu. A. Guryan, Nature (London) **282**, 587 (1979).
- (3) K. Hurley, T. Cline, E. Mazets, S. Barthelmy, P. Butterworth, F. Marshall, D. Palmer, R. Aptekar, S. Golenetskii, V. Il'inskii, D. Frederiks, J. McTiernan, R. Gold, and J. Trombka, Nature (London) **397**, 41 (1999).
- (4) C. Kouveliotou, S. Dieters, T. Strohmayer, J. van Paradijs, G. J. Fishman, C. A. Meegan, K. Hurley, J. Kommers, I. Smith, D. Frail, and T. Murakami, Nature (London) **393**, 235 (1998).
- (5) C. Kouveliotou, T. Strohmayer, K. Hurley, J. van Paradijs, M. H. Finger, S. Dieters, P. Woods, C. Thompson, and R. C. Duncan, Astrophys. J. **510**, L115 (1999); T. Murakami, S. Kubo, N. Shibazaki, T. Takeshima, A. Yoshida, and N. Kawai, Astrophys. J. **510**, L119 (1999).
- (6) E. V. Gotthelf, G. Vasisht, and T. Dotani, Astrophys. J. **522**, L49 (1999).
- (7) V. M. Kaspi, D. Chakrabarty, and J. Steinberger, Astrophys. J. **525**, L33 (1999).
- (8) R. C. Duncan and C. Thompson, Astrophys. J. **392**, L9 (1992).
- (9) C. Thompson and R. C. Duncan, Mon. Not. R. Astron. Soc. **275**, 255 (1995); Astrophys. J. **473**, 322 (1996).
- (10) C. Thompson and N. Murray, Astrophys. J. **560**, 339 (2001).
- (11) V. N. Kondratyev, JAERI-Research 2001-057 (2001).
- (12) V. N. Kondratyev, JAERI-Conf 2001-12, 14 (2001); Phys. Rev. Lett. **88**, 221101 (2002).
- (13) S. L. Shapiro and S. A. Teukolsky, *Black Holes, White Dwarfs, and Neutron Stars* (Wiley, New York, 1983).
- (14) P. Haensel, J. L. Zdunik, and J. Dobaczewski, Astron. Astrophys. **222**, 353 (1989).
- (15) K. Oyamatsu and M. Yamada, Nucl. Phys. A **578**, 181 (1994).
- (16) C. J. Pethick and D. G. Ravenhall, Ann. Rev. Nucl. Part. Sci. **45**, 429 (1995).
- (17) F. Douchin, P. Haensel, and J. Meyer, Nucl. Phys. A **665**, 419 (2000).
- (18) G. Audi and A. H. Wapstra, Nucl. Phys. A **595**, 409 (1995).
- (19) A. Broderick, M. Prakash, and J. M. Lattimer, Astrophys. J. **537**, 351 (2000).
- (20) A. Bohr and B. R. Mottelson, *Nuclear Structure* (Benjamin, NY, 1969).
- (21) S. G. Nilsson and I. Ragnarsson, *Shapes and Shells in Nuclear Structure* (Cambridge Univ. Press, Cambridge, 1990).
- (22) J. A. van Leeuwen, J. Phys. (Paris) **2**, 361 (1921); Ya. P. Terletskii, Zhurn. Eksp. Teor. Fiz. **9**, 796 (1939).
- (23) V. M. Strutinsky, Nucl. Phys. A **95**, 420 (1967); Nucl. Phys. A **122**, 1 (1968).
- (24) V. N. Kondratyev and H. O. Lutz, Phys. Rev. Lett. **81**, 4508 (1998); Eur. Phys. J. D **9**, 483 (1999).
- (25) W. A. Fowler, Rev. Mod. Phys. **56**, 149 (1984).